A Theoretical Case Study of Type I and Type II β-Turns**

Eszter Czinki,[a] Attila G. Császár,*[a] and András Perczel[b]

Abstract: NMR chemical shielding anisotropy tensors have been computed by employing a medium size basis set and the GIAO-DFT(B3LYP) formalism of electronic structure theory for all of the atoms of type I and type II β-turn models. The models contain all possible combinations of the amino acid residues Gly, Ala, Val, and Ser, with all possible side-chain orientations where applicable in a dipeptide. The several hundred structures investigated contain either constrained or optimized ϕ, ψ, and χ dihedral angles. A statistical analysis of the resulting large database was performed and multidimensional (2D and 3D) chemical-shift/chemical-shift plots were generated. The $^{1}H^{\alpha}$-$^{13}C^{\alpha}$, $^{13}C^{\alpha}$-$1H^{\alpha}$-$^{13}C^{\beta}$, and $^{13}C^{\alpha}$-$^{1}H^{\alpha}$-$^{13}C'$ 2D and 3D plots have the notable feature that the conformers clearly cluster in distinct regions. This allows straightforward identification of the backbone and side-chain conformations of the residues forming β-turns. Chemical shift calculations on larger For-(L-Ala)$_n$-NH_2 ($n = 4$, 6, 8) models, containing a single type I or type II β-turn, prove that the simple models employed are adequate. A limited number of chemical shift calculations performed at the highly correlated CCSD(T) level prove the adequacy of the computational method chosen. For all nuclei, statistically averaged theoretical and experimental shifts taken from the BioMagnetic Resonance Bank (BMRB) exhibit good correlation. These results confirm and extend our previous findings that chemical shift information from selected multiple-pulse NMR experiments could be employed directly to extract folding information for polypeptides and proteins.

Keywords: ab initio calculations · beta turn · chemical shift · peptides · structure elucidation

Introduction

Relative orientations within the backbone of a protein, (see Figure 1 for a schematic representation of constituent atoms and typical dihedral angles[1] in proteins) which are also influenced by appropriate side chains, determine its global fold. Determination of the 3D structure of peptides and small proteins from NMR experiments has been based primarily on the extraction of distance-type constraints, mostly proton–proton distances from nuclear overhauser exchange spectroscopy (NOESY).[2–10] For a successful 3D structure determination by NMR spectroscopy it is mandatory to assign all resonances. To achieve full resonance assignment for unlabeled and singly-labeled (^{15}N) proteins, *J*-correlated spectra and NOESY-type information are essential. On the other hand, if a doubly-labeled (^{13}C and ^{15}N) protein is made available, the full assignment can be achieved without NOE-type information by using specifically designed experiments, and by exploring homo- and heteronuclear coupling constants.[8–10] At present, however, even if all the assignments are correctly determined from *J*-correlated spectroscopic data, the 3D structure of the molecule cannot be determined without the analysis of the information derived from NOESY-type spectra.

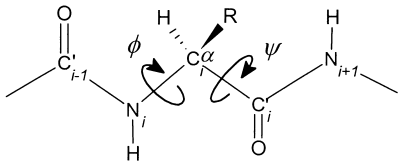

Figure 1. Typical dihedral angles, ϕ ($C'_{i-1}-N_i-C^{\alpha}_i-C'_i$) and ψ ($N_i-C^{\alpha}_i-C'_i-N_{i+1}$), of proteins represented in a simple peptide model.

Chemical shielding of a nucleus, located in different proteins or at different sites within the same protein, changes as a function of the individual molecular surrounding within the macromolecule or differences in backbone orientations. If the latter factor is the dominant one, the local fold of protein subunits can be revealed from chemical-shift information

[a] Prof. A. G. Császár, E. Czinki
Department of Theoretical Chemistry
Eötvös University, 1518 Budapest 112
P.O. Box 32 (Hungary)
Fax: (+36) 1209-0602
E-mail: csaszar@chem.elte.hu, czinki@chem.elte.hu

[b] Prof. A. Perczel
Department of Organic Chemistry
Eötvös University, 1518 Budapest 112
P.O. Box 32 (Hungary)
Fax: (+36) 1209-0602
E-mail: perczel@para.chem.elte.hu

[**] Toward Direct Determination of Conformations of Protein Building Units from Multidimensional NMR Experiments, Part IV; for part III see: *Eur. Phys. J. D* **2002**, *20*, 573

Supporting information for this article is available on the WWW under http://www.chemeuj.org or from the author.

0947-6539/03/0905-1182 $ 20.00+.50/0

alone. Indeed, numerous NMR experiments[11–19] as well as theoretical studies[20–28] appeared which were designed to find an alternative to NOE-based structural determination of biomolecules. These studies are all based on the assumption that the chemical shift of a particular nucleus X in a protein of 3D structure **R** is written as:

$$\delta^{X}(\mathbf{R}) = \Delta\delta^{X}(\mathbf{R}) + \delta^{X}_{rc}(\mathbf{R}) \quad (1)$$

In Equation (1) δ_{rc} and $\Delta\delta$ stand for the random-coil and structural shift values, respectively, that is, δ_{rc} does not directly contain spatial information. Empirical random-coil values can be determined from investigation of NMR databases, for example, the BioMagnetic Resonance Bank, BMRB,[29] or directly from experiments. Theoretical random-coil values at a given level of theory can be determined by using energy-weighted and energy-unweighted schemes. Apart from $^{1}H^{N}$, the values agree surprisingly well with the well-established empirical values.[22–24] The structural shift can be given as Equation (2):

$$\delta^{X}(\mathbf{R}) = \Delta\delta^{X}_{local}(\mathbf{R}) + \Delta\delta^{X}_{nonlocal}(\mathbf{R}) \quad (2)$$

In order for structure determinations based on chemical shifts to be successful the local effect should dominate.

Systematic theoretical investigations of "monopeptides" and scattered studies on oligopeptides, as well as relevant experiments, have offered several interesting results. Different nuclei respond vastly differently to structural changes; for example, the appropriate ^{1}H, ^{13}C, ^{17}O, and ^{15}N chemical shift ranges are about 2, 8, 10, and 25 ppm, respectively.[17] There is a characteristic shift of $^{15}N^{H}$ in Gly, Ser, and Thr residues.[26] Multidimensional NMR experiments[12] have established a few structure-induced $^{13}C^{\alpha}$, $^{15}N^{H}$, and $^{1}H^{N}$ chemical shift changes in peptides and proteins, providing correlation examples of backbone folds of peptides and proteins with NMR chemical shifts. These results provided hope that direct analysis of NMR chemical shifts from relevant multiple-pulse experiments (e.g., 2D-HMQC,[30] 2D-HSQC,[31] and 3D-HNCA[32]) may prove to be a plausible alternative to the distance-based (NOE) strategy for elucidation of the dihedral space of protein structures. It became well known from different ^{1}H-X-type correlated NMR experiments (e.g., $^{1}H^{N}$-^{15}N HSQC) that ^{15}N chemical shifts are rather sensitive probes of protein main-chain fold and have considerable potential for structure determination. Nevertheless, due to their fairly complex dependence on several torsion angles and on electrostatic field effects,[26] interpretation of changes in ^{15}N shifts proved to be somewhat more complicated than that of changes in ^{13}C shifts. In short, while the most important structural factors determining the ^{15}N NMR chemical shift of amino acid residue *i* appear to be the dihedral angles ψ_{i-1} and ϕ_i, the angles ψ_i and ϕ_{i-1}, and the side-chain orientation also have an effect. Consequently, at present ^{15}N shifts appear to be less useful than ^{13}C shifts. It was found[26] computationally that $^{13}C^{\alpha}$ values in helices and strands are shifted by $\approx$2.3 ppm downfield and $\approx$2.9 ppm upfield, respectively, as compared to the random coil value. These shifts should be compared with available experimental results,[27] about +3.2 ppm and −1.2 ppm, respectively. For all residues studied, the $^{13}C^{\alpha}$ shift showed the expected $\approx$5 ppm increase for the β conformation over the helical structure. Furthermore, the diagonal CSA tensor elements were all found to be sensitive to changes in the ϕ, ψ, and χ_1 torsion angles. It is well known that in the strands of β-hairpin motifs the $^{13}C^{\alpha}$ conformational shifts are negative and the $^{13}C^{\beta}$ conformational shifts are positive. Hydrogen bonds have a crucial role in the formation and stabilization of peptides and proteins. For example, Asakawa and co-workers[33] found that the C^{α} shielding values are affected not only by the values of the torsional parameters (ϕ, ψ), but also by hydrogen-bond patterns (standard, bifurcated, etc.) and by hydrogen-bond strength. This observation proved to be crucial during determination of the 3D structure of ribonuclease and that of a basic pancreatic trypsin inhibitor.[33] GIAO-RHF calculations also established the influence of hydrogen bonding on the carbonyl carbon of *N*-methylacetamide interacting with formamide.[34] Further computations at the 6-31G** GIAO-RHF level have been performed on the helical and β-sheet structures of For-$(Ala)_5$-NH_2 in order to investigate the effect of intramolecular hydrogen bonds on shieldings of different nuclei, for example, $^{13}C'$.[34] The experimentally determined difference between the helical and the β-sheet values of $^{13}C'$, 4.6 ppm, is close to the calculated value, 4.9 ppm. The most significant perturbation caused by the hydrogen bond was on carbonyl carbons.[35] Laws and co-workers[36] have determined the effect of basis set extension at the GIAO-RHF level, by employing standard

Abstract in Hungarian: *A GIAO-DFT(B3LYP) formalizmus és közepes méretű bázis segítségével NMR árnyékolási tenzor számításokat végeztünk az I-es és II-es típusú β-kanyarok összes atomjára. A dipeptid β-kanyar modellek Gly, Ala, Val és Ser aminosavakat tartalmaztak az összes lehetséges kombinációban, a Val és Ser esetén a lehetséges oldallánc-orientációk figyelembe vétele mellett. A vizsgált több száz modellt rőgzített ill. optimált ϕ és ψ diéderes szögek jellemzik. Elvégeztük a létrejött hatalmas adatbázis statisztikai elemzését és több-dimenziós (2D és 3D) kémiai eltolódás- kémiai eltolódás korrelációs térképeket készítettünk. A $^{1}H^{\alpha}$-$^{13}C^{\alpha}$ és $^{13}C^{\alpha}$-$^{1}H^{\alpha}$-$^{13}C^{\beta}$, $^{13}C^{\alpha}$-$^{1}H^{\alpha}$-C′ 2D és 3D térképek fontos sajátsága, hogy a különböző konformerek egyértelműen elkülönült régiókat alkotnak. Ez a sajátság a β-kanyarokat alkotó aminosavak gerinc- (és sok esetben az oldallánc-) konformereinek egyértelmő meghatározását teszi lehetővé. A választott modell megfelelöségét a nagyobb For-(L-Ala)$_n$-NH$_2$ (n = 4, 6, 8) modellekre - melyek I-es és II-es típusú β-kanyarokat tartalmaztak - végzett kémiai eltolódás számítások eredményei bizonyítják. A számítási eljárás megfelelőségét az elektron-korrelációt magas szinten figyelembe vevő GIAO-CCSD(T) szinten számított kémiai eltolódás értékek támasztják alá. Az elméleti és kísérleti (a BioMagneticResonanceBank-ban (BMRB) elhelyezett) kémiai eltolódás értékek statisztikai átlagai minden magra kiváló korrelációt mutatnak. Az új eredmények megerősítik és egyben kiterjesztik korábbi megfigyelésünket: helyesen kiválasztott több-dimenziós NMR mérésekből adódó kémiai eltolódás értékek közvetlenül alkalmazhatók polipeptidek és proteinek térszerkezetének meghatározására.*

  0947-6539/03/0905-1183 $ 20.00+.50/0

basis sets STO-3G, 3-21G, 4-31G, and 6-311 + G(2d) on $^{13}C^{\alpha}$ and $^{13}C^{\beta}$ shifts of two amino acid residues, Ala and Val, in proteins. They found that the chemical shifts of these residues, determined by using smaller basis sets, correlate rather well with results obtained with larger basis sets, even when the underlying reference geometries were slightly different. It is encouraging that chemical shifts computed at different levels can be scaled.

Establishment of these results led to program developments and to further tests on proteins. Several empirical programs have been developed, such as CAMRA[37] and TALOS,[38] which use a chemical shift database from homologous proteins to make NMR assignments in proteins. Focusing on Ala and Val residues, Pearson et al. found that in a protein such as nuclease, the ϕ and ψ values can be estimated using chemical shifts.[39] Although the results obtained are less dependable than those derived from NOEs and *J*-coupling constraints, the strategy seemed very promising for the estimation of secondary structures. Analyzing chemical shift nonequivalencies of Ala and Val residues in proteins like calmodulin and nuclease, the applicability of the direct strategy was further explored.[16c] Prompted by these results, ^{13}C CSA tensor computations were extended[40] to cover additional amino acid residues, such as Ile, Ser, and Thr. When studying ^{15}N shifts for bovine pancreatic trypsin inhibitor and apamin, Gluska and co-workers,[18] showed a correlation between the ψ_{i-1} angle and ^{15}N shifts for β-sheet residues but little other useful information. Celda et al.[13] utilized correlations of C^{α} structural shifts to refine the NMR structure of epidermal growth factor, a small protein containing 53 amino acids. Le and Oldfield[20] studied the amide ^{15}N shifts in 14 proteins and seem to have found an empirical correlation between ^{15}N shifts and the ϕ_i and ψ_{i-1} dihedral angles. Overall, it seems that chemical shift results from 1D NMR experiments are not sufficient for 3D structure elucidation of larger biomolecules, even if they have relatively rigid structures. In a further study of relevance, an attempt was made to predict ^{13}C shift values of valine residues in three well-known proteins (calmoduline, nuclease, and ubiquitine)[41] by employing empirical chemical shift surfaces and utilizing their X-ray structures. Most Hartree–Fock (HF) results and experimental values showed agreement[41] poorer than expected, but the agreement improved slightly by using density functional theory (DFT) calculations. Pearson and coworkers[41] have thus concluded that for accurate computation of chemical shifts, geometry optimization and the inclusion of electron correlation in the theoretical treatment appear to be important.

In summary, all calculations and most experiments indicate that it is possible to deduce certain backbone and side-chain orientations from chemical shift data alone.

After completing systematic ab initio studies of NMR chemical shifts of simple monopeptide (diamide) models,[22–24] in this study we now start extending our approach to larger peptide models, in particular to β-turns.

In globular proteins the third most important secondary structure element, after α-helices and β-pleated sheets, is the β-turn. The simplest and most abundant β-turns, those of type I and type II,[42] can be characterized by using only two residues, $i + 1$ and $i + 2$, in the middle of a turn. Therefore, it was natural to start the theoretical NMR shielding study of secondary structural elements with these important building units.

According to the traditional definition of Venkatachalam,[42] β-turns can be characterized by the ϕ and ψ torsional angles of the two residues in the middle of the turn. Later this definition was extended by a distance criterion,[43] according to which the C_i^{α}-C_{i+3}^{α} distance must be shorter than 7 Å. Although β-turns are mostly stabilized by hydrogen bonds, it has not been proven that such hydrogen bonds are necessary requirements of the appearance of β-turns. The dihedral angles characteristic of type I β-turns are as follows: $\phi_{i+1} \approx -60^{\circ} \pm 30^{\circ}$, $\psi_{i+1} \approx -30^{\circ} \pm 30^{\circ}$, $\phi_{i+2} \approx -90^{\circ} \pm 30^{\circ}$, $\psi_{i+2} \approx 0^{\circ} \pm 50^{\circ}$. In our notation[44] these dihedral angles correspond to conformer $\alpha_L\delta_L$. The dihedral angles characteristic of type II β-turns are as follows: $\phi_{i+1} \approx -60^{\circ} \pm 30^{\circ}$, $\psi_{i+1} \approx 120^{\circ} \pm 30^{\circ}$, $\phi_{i+2} \approx 80^{\circ} \pm 30^{\circ}$, $\psi_{i+2} \approx 0^{\circ} \pm 50^{\circ}$ (conformer $\varepsilon_L\alpha_D$ in our notation). These conformer names will be used throughout this paper.

Investigation of the structural and NMR properties of β-turns is important, since they determine hairpin stability, β-strand alignment in β-hairpins, and connecting and fixing secondary structural elements of a periodic nature. The biological role of β-turns is also important. These motifs often end up at the surface of proteins where they are responsible for important biochemical processes, like post-translational modifications (glycosylation, phosphorylation), immunrecognition, and so on.

The dipeptide model system as part of typical type I and type II β-turns of an octapeptide model made up of Ala residues is depicted in Figure 2. Our basic β-turn model, For-

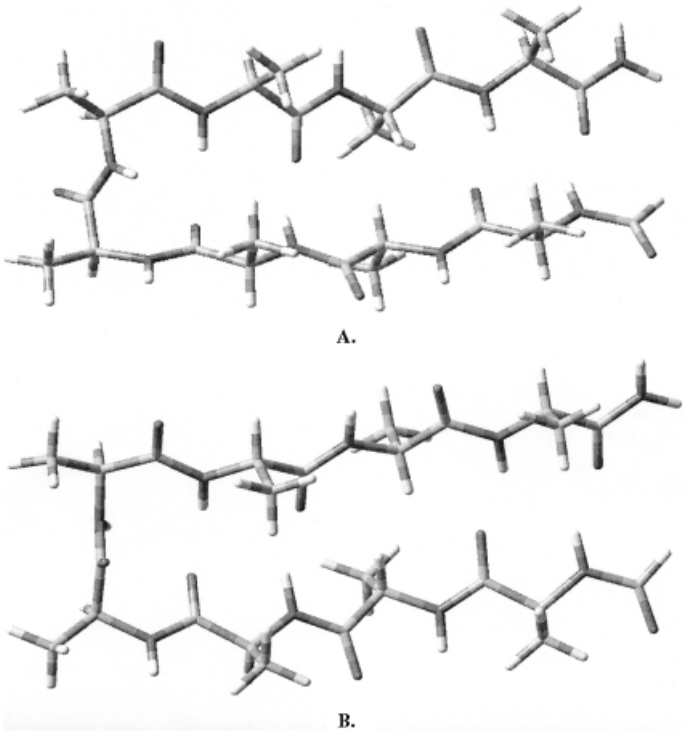

Figure 2. Type I (A) and type II (B) β-turn structures in For–(L–Ala)$_8$–NH_2 models.

0947-6539/03/0905-1184 $ 20.00+.50/0 *Chem. Eur. J.* **2003**, *9*, No. 5

Xxx-Yyy-NH_2, contains two amino acids Xxx and Yyy, a formyl (For) group, and an amide group at the ends. The amino acids Gly, Ala, Val, and Ser were chosen for modeling of the naturally most abundant type I and type II β-turns. For the sake of completeness, all four amino acids are placed into both positions of both types of β-turns. The choice of the amino acid residues was based on the following considerations:

a) Ala is the simplest chiral amino acid and therefore most of the experimental and theoretical structural studies contain it as the main building block of any structural motif.
b) Hydrophobic amino acid residues are found most often in the $(i+1)$ position of β-turns. Therefore, Ala and Val as the simplest residues with apolar side chains are especially important, and at the same time are the easiest to compute.
c) If Gly is found in the second $(i+2)$ position of a β-turn it almost always leads to a type II structure. Obviously Gly, as the simplest, achiral amino acid is especially suitable for a systematic ab initio investigation.
d) If Ser is in the $(i+2)$ position of a β-turn, one almost exclusively finds in nature a type I structure. Furthermore, Ser is the simplest residue with a polar side chain that can form hydrogen bonds. Study of the Val and Ser residues also provides insight into the effect the side chain has on chemical shifts in the backbone.

In this paper a library of calculated geometric parameters and chemical shifts is established for the β-turn structural unit of peptides. The detailed structural analysis of β-turn models is published elsewhere.[45] Partly due to the lack of detailed experimental information on these systems, it is not evident what is the best use of the large number of quantum chemical data in the library. As in our previous studies,[22–24] we feel that a thorough statistical analysis, even in its simplest linearized form, offers the best way to confirm existing structure/structure, structure/chemical shift, and chemical-shift/chemical-shift correlations, and derive new ones. Therefore, a concerted attempt has been made to correlate calculated isotropic NMR shielding and the resulting chemical shift values with *all* characteristic backbone conformations.

Computational Methods

The reference geometries of β-turn models employed for the NMR shielding tensor computations of this study have been determined at the 3-21G RHF level. The geometry optimizations were carried out using the Gaussian 98 program system.[46] Part of the relevant results are reported in reference [45]. Due to the large number of side-chain conformers considered, the geometry optimizations resulted in more than 200 structures; this means that the subsequent NMR calculations resulted in chemical shift data for all the atoms of more than 400 residues. Extraction of structural and chemical shift information, from the large number of output files, was made by a program written in Python,[47] while extraction of useful chemical information from this database was made by a careful statistical analysis of the data.[48]

Computation of NMR shielding tensors presented in this study used the Gaussian 98[46] and AcesII[49] program systems. The NMR shielding tensor calculations were performed at the GIAO-RHF[50, 51] (gauge including atomic orbitals restricted Hartree–Fock), GIAO-DFT(B3LYP) (GIAO density functional theory by employing the Becke3–Lee–Yang–Parr functional[52]), GIAO-MP2[53] (GIAO second-order Møller-Plesset perturbation theory), GIAO-CCSD[54] (GIAO coupled cluster theory with single and double substitution), and GIAO-CCSD(T)[55] (GIAO CC theory with single, double, and estimated triple substitution) levels of theory. The basis sets employed included the 6-311++G**,[56] the pVDZ,[57] and the TZ2P[58] sets. The last basis set was the same as employed in our previous studies of the same nature.[22–24] In order to allow the use of relative chemical shifts (δ-scale), the appropriate isotropic chemical shielding values of ^{1}H, ^{13}C, and ^{15}N were referenced to ^{1}H and ^{13}C of tetramethylsilane (TMS), and to ^{15}N of NH_3. The reference geometry chosen for NH_3 corresponded to the all-electron aug-cc-pVTZ CCSD(T) optimized geometry,[59] while the geometry of TMS has been optimized at the 6-311++G** B3LYP level.

There are several factors determining the accuracy of computed NMR shieldings: choice of the model, quality of the underlying reference geometries, effect of one-particle basis set deficiency, and the extent of electron correlation. Previously, we revealed that the conformers of diamide models are clearly distinguishable on certain chemical shift-chemical shift correlated plots independent of the basis set employed for the calculation of the chemical shieldings. [22–24] Although the choice of whether the GIAO-RHF calculations were performed at constrained or fully optimized reference geometries has an effect on the calculated shieldings, separation of the backbone conformers on these plots was clearly not affected.

It is worth discussing how the dipeptide models we chose for this study represent naturally occuring β-turns. To test the effect of the length of the peptide chain on chemical shift values, NMR shielding computations have been performed for the appropriate conformers of the models, For-(L-Ala)$_n$-NH_2 ($n=4$, 6, and 8), with structures optimized at the 3-21G RHF level taken from reference [45](note that NMR shift differences between the dipeptide and larger models are thus not only due to the different lengths of the models but are also to dihedral angle differences). Figure 8 (see below) shows that the length of the model changes the computed chemical shifts very little, supporting the choice of the dipeptide model for this study; also the shift values of the $n=6$ and 8 models basically coincide.

To test the effect of electron correlation on NMR shielding constants for peptide models high level computations (GIAO-MP2, GIAO-CCSD, and GIAO-CCSD(T)) were performed for the For-Gly-NH_2 diamide model by employing a pVDZ basis set. The results obtained are presented in Table 1.

Table 1. Differences of NMR chemical shifts obtained at the GIAO-pVDZ RHF, GIAO-B3LYP, GIAO-MP2, GIAO-CCSD, and GIAO-CCSD(T) levels between the extended (β_{LD}) and γ-turn (γ_{LD}) conformers of For-Gly-NH_2[a].

	CCSD(T)-RHF	CCSD(T)-B3LYP	CCSD(T)-MP2	CCSD(T)-CCSD
$^{13}C^{\alpha}$	1.30	0.39	−0.31	0.31
$^{1}H^{\alpha}$	−0.21	0.15	0.01	−0.04
$^{1}H^{\alpha}$	0.11	−0.03	−0.02	0.03
$^{14}N^{H}$	0.71	0.61	−0.05	0.26
$^{1}H^{N}$	0.40	0.04	−0.06	0.06

[a] All values are in ppm.

Analyzing the difference of calculated NMR shifts of the two conformers (β and γ), one can see that the difference between CCSD(T) and RHF results are the largest, and the difference between CCSD(T) and MP2 results are the smallest. Although the B3LYP method incorporates some electron correlation, from our limited test results it is evident that it provides less accurate results than the MP2 method. Nevertheless, B3LYP results show considerable improvement over RHF results and this level is certainly affordable for much larger systems.

Our previous findings revealed that the absolute RHF chemical shift values of certain nuclei (e.g., $^{15}N^{H}$ and $^{1}H^{N}$) deviate considerably from the experimental data.[22–24] The reason for this discrepancy, however, is not due to the lack of electron correlation. The CCSD(T) values are just as far from the experimental values as the RHF data.

In order to facilitate comparison of NMR shielding results obtained at different computational levels, we calculated isotropic shieldings for For-L-Ala-NH_2 with the 6-311++G(d,p) and TZ2P basis sets both at the RHF and DFT(B3LYP) levels of theory. The results can be compared to experimental data deposited in the database of Wishart et al.[60] Since not

enough experimental data is available, only the $^1H^\alpha$ and $^{13}C^\alpha$ NMR shift data of the Ala residue can be compared. Table 2 lists the average differences of the calculated and experimental data. It is clear that the TZ2P B3LYP level gives the best chemical shift results.

Table 2. Average difference of the calculated and experimental $^{13}C^\alpha$ and $^1H^\alpha$ NMR chemical shifts for each conformer of the For-L-Ala-NH_2 model peptide.[a]

Level of theory	$\delta(^1H^\alpha)_{exptl} - \delta(^1H\alpha)_{calcd}$	$\delta(^{13}C\alpha)_{exptl} - \delta(^{13}C\alpha)_{calcd}$
6-311++G(d,p) RHF	0.59	3.35
TZ2P RHF	0.71	3.90
6-311++G(d,p) B3LYP	1.06	5.22
TZ2P B3LYP	0.43	2.33

[a] The underlying experimental averages refer to the database of Wishart. The calculated averages include all major conformers of For-L-Ala-NH_2.

The average of computed chemical shifts was compared to experimental average (the BMRB[29]) values for each amino acid. The goodness-of-fit factors of linear regression for $^1H^\alpha$, $^1H^N$, $^{13}C^\alpha$, $^{13}C'$, and $^{15}N^H$ chemical shifts was higher than 0.994 for all four amino acids.

Chemical-shift values of all β-turn secondary structures associated with any of our model systems were retrieved from the database of Wishart et al.,[60] which contains NMR shifts of 18 proteins, and have been compared to our calculated values. The calculated $^1H^\alpha$ and $^{13}C^\alpha$ chemical shifts, if experimental counterpart available, show significant correlation.

All relevant structural and chemical shift data for all fully optimized structures are deposited in the Supporting Information.

Results and Discussion

Structures and energetics: As noted in the Introduction, a type I β-turn has $\alpha_L\delta_L$ conformation that is not changed due to the modifying effect of side chains.[61] In our β-turn models the α_L region is found to be rather narrow, and instead of being centrosymmetric, it is shaped like a valley (see Figure 3) that

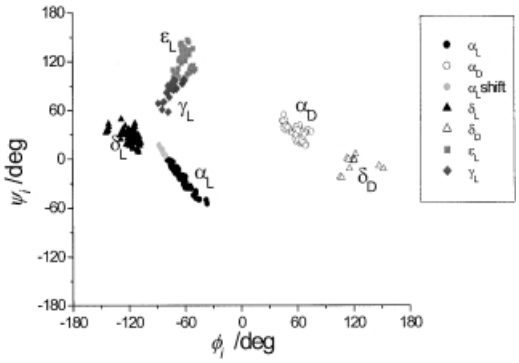

Figure 3. Residues of type I ($\alpha_L\alpha_L$) and type II ($\varepsilon_L\alpha_D$, $\varepsilon_L\delta_D$, $\gamma_L\alpha_D$, $\gamma_L\gamma_D$) β-turns, optimized at the 3-21G RHF level, on a Ramachandran-type (ϕ_i, ψ_i) plot.

extends toward the neighboring δ_L region (shown on Figure 3 as an α_L-shift). In the case of type II β-turns, $\varepsilon_L\alpha_D$, the following subtypes have been observed: a) the first subunit may have a γ_L conformation, since ε_L and γ_L are neighboring regions on the Ramachandran surface; and b) in the case of the For-Xxx-Gly-NH_2 models, the second subunit may have a conformation that is better described as δ_D (α_D and δ_D are also neighboring regions).[61]

When our β-turn model contains Ser, certain side-chain orientations are not found to be minima. If Ser is the second subunit, all optimizations starting from the *aa* and *ag*+ side-chain orientations end up with an *ag*− side-chain orientation. (For labeling of side-chain orientations the following abbreviations are employed: {*a*,*g*+,*g*−} refer to χ angles of {180°, 60°, −60°}, where *a* and *g* stand for *anti* and *gauche*, respectively.) The reason for this is most likely the establishment of a hydrogen bond between the O–H of Ser and the O atom of the C terminus.

In four cases our optimization procedures resulted in two stable conformers with slightly different torsional angles in the γ_L region (see Figures 7–10). Consequently, we have two stable $\gamma_L\alpha_D$ models with slightly different ϕ and ψ dihedral angles. Due to the strong dependence of chemical shifts on ϕ and ψ, these conformers, indicated on Figures 7–10 (below) as $(\gamma_L\alpha_D)^2$*, have slightly different chemical shifts.

It is not the purpose of this paper to discuss energetic features of the investigated model compounds at length, for more details see reference [45].

Raw model—fixed ϕ, ψ, and χ dihedral angles: The main aim of this study is to establish chemical-shift/dihedral-angle correlations in β-turns. In a raw, "idealized" model occurrences of such relationships are investigated by keeping the important dihedral angles of the residues constant at their well-established mean values (see Computational Methods), while optimizing all other geometry parameters. In order to minimize other existing effects (e.g., hydrogen bond, dipole, and side-chain interaction effects), the χ torsional angles for Ser and Val had to be fixed. We chose side-chain orientations in which the backbone and side-chain interactions do not have to be taken into consideration. (Val: $\chi \approx 180°$ in all cases; Ser: $i+1$: χ_1: *a*, χ_2: *a*, $i+2$: χ_1: *g*−, χ_2: *a* in both types of β-turns.) NMR shielding calculations at the usual TZ2P B3LYP-GIAO level were performed at these constrained geometries. If no chemical-shift/structure correlations are observed in such simplified models, it is unlikely that they will exist in more complex models or in real systems. Subsequent relaxation of the structural constraints would allow exploration of effects disturbing the observed correlations.

In Figure 4, $^1H^\alpha$-$^{13}C^\alpha$ correlations are presented for the four residues investigated, Gly, Ala, Val, and Ser, placed both at the ($i+1$) and ($i+2$) positions of the β-turn. (Note that other correlation plots have also been generated with similar characteristics, but the $^1H^\alpha$-$^{13}C^\alpha$ correlations are the most significant, and thus they are the only ones presented.) These figures prove beyond reasonable doubt that, to the great advantage of NMR structural determination of peptides and proteins, the most important factor determining the position of the conformers on this chemical-shift/chemical-shift plot is the backbone structure. In other words, for all four residues investigated the different backbone orientations cluster in significantly different regions, allowing straightforward and unambiguous identification of the subconformers α_L, δ_L, ε_L, and α_D, and thus both types of β-turns. Figure 4 also shows that the neighboring amino acid has only a small effect on the

0947-6539/03/0905-1186 $ 20.00+.50/0 *Chem. Eur. J.* **2003**, *9*, No. 5

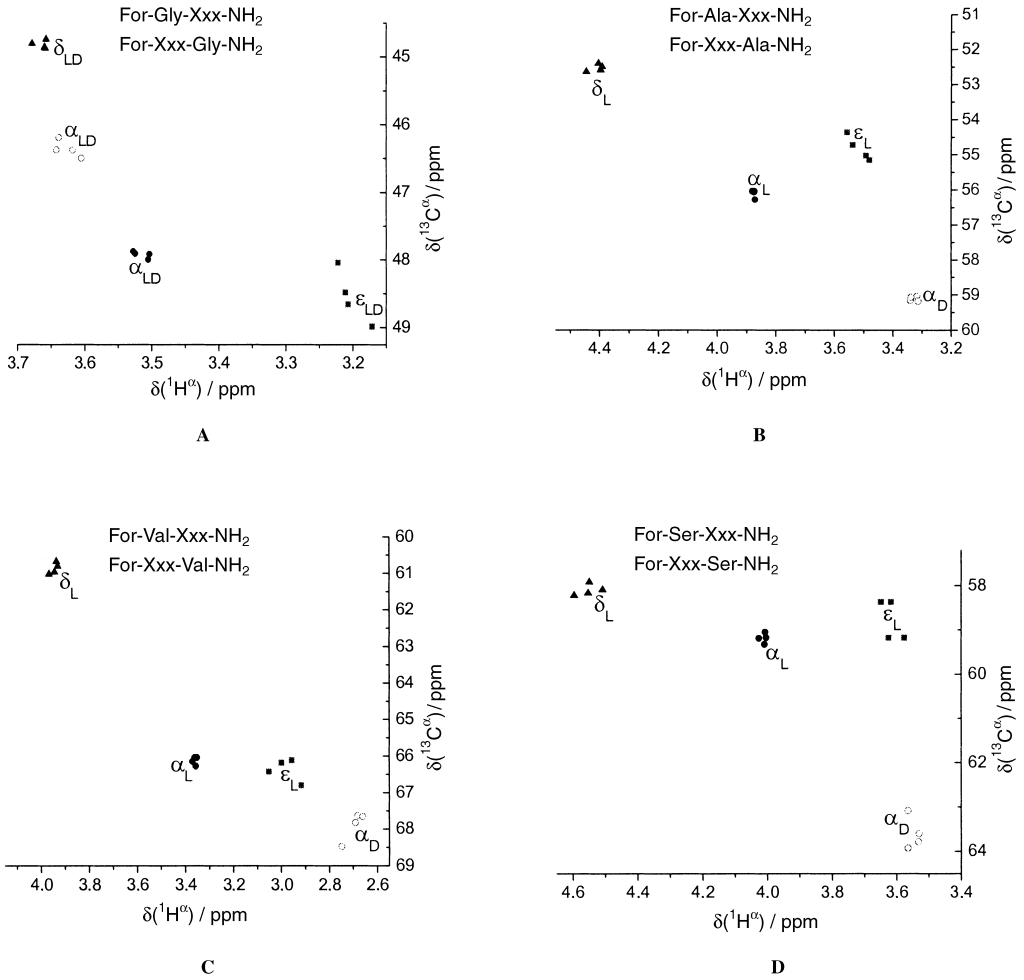

Figure 4. Appropriate chemical shifts of Gly (A), Ala (B), Val (C) and Ser (D) residues on $^{1}H^{\alpha}$-$^{13}C^{\alpha}$ correlation plots for raw models (fixed ϕ, ψ and χ dihedral angles).

arrangements of the points on the plots. The next important observation is that these regions are located at somewhat different positions for the individual residues; thus even in this simplified model, no residue-independent characteristics can be offered for structural studies using chemical-shift/chemical-shift correlation plots. The last notable conclusion is that once the backbone angles of the residues are fixed, the scatter of the points on the $^{1}H^{\alpha}$-$^{13}C^{\alpha}$ correlation plots is extremely small. In summary, NMR correlation plots should serve as tools of considerable utility for the determination of the 3D structures of peptides and should supplement NOE-type studies.

It is only natural to extend our study from here to fully optimized structures, which will be the subject of the next section. Since optimized and constrained backbone angles usually differ by less than 10°, it is not expected that the extremely pleasing results found in this section will be greatly affected. No linear relation is expected for the deviations induced by diverse structural effects.

Chemical-shift/chemical-shift correlations: It soon became clear from our present and previous[22–24] studies that one-dimensional chemical-shift/torsion-angle plots do not provide enough information to determine the torsional preference of amino acid residues. On the other hand, two- and three-dimensional chemical-shift/chemical-shift correlation maps do provide the required information, perhaps even for the side chains, as shown in this and the previous sections. Such maps may be considered as analogues of results from the nowadays popular and routine multidimensional NMR experiments. From the many possible homo- and heteronuclear correlation plots investigated it was found that the $^{1}H^{\alpha}$-$^{13}C^{\alpha}$ 2D, $^{13}C^{\alpha}$-$^{1}H^{\alpha}$-$^{13}C^{\beta}$, and $^{13}C^{\alpha}$-$^{1}H^{\alpha}$-$^{13}C'$ 3D maps are of highest relevance for structural studies, and thus only these are discussed, separately below.

$^{1}H^{\alpha}$-$^{13}C^{\alpha}$ plots: In these plots, analogous to the results of basic heteronuclear correlation experiments (e.g., 2D HSQC, maps [8, 10]), the different conformers form separated clusters. Statistically speaking, the Pearson correlation coefficients[48] for these data pairs are among the highest observed in our studies.

Due to the achirality of the Gly residue, the L and D mirror image conformers have the same chemical shift values. The reduced number of conformer types cluster on the $^{1}H^{\alpha}$-$^{13}C^{\alpha}$ correlation map (see Figure 5). Figure 5 clearly shows whether Gly is in the first or second position of the β-turn, and whether it is in a type I or type II form.

  0947-6539/03/0905-1187 $ 20.00+.50/0

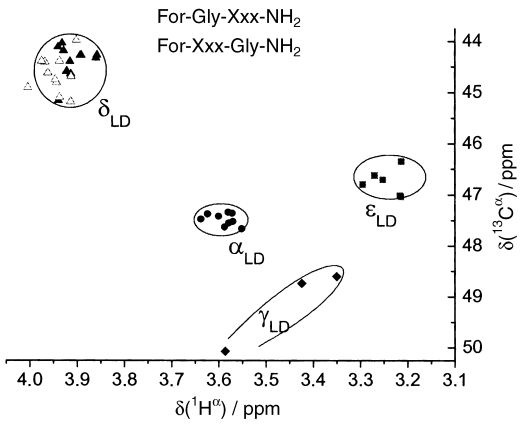

Figure 5. $^{1}H^{\alpha}$-$^{13}C^{\alpha}$ chemical-shift/chemical-shift correlation map for Gly residues in both positions.

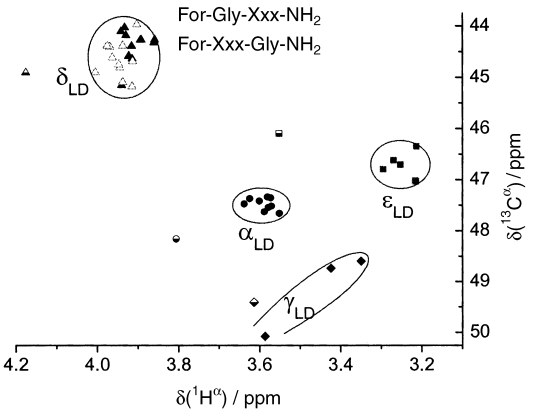

Figure 6. $^{1}H^{\alpha}$-$^{13}C^{\alpha}$ chemical shift correlation map for Gly residues in both positions. NMR shifts calculated for β-turn structures optimized at the 6-311++G(d,p) RHF level are indicated by half hollow symbols.

The effect of basis set enlargement at the RHF level on the NMR chemical shifts was examined for the Gly residue, the only achiral amino acid. Figure 6 shows that the qualitative appearance (i.e., separated conformers) of the $^{1}H^{\alpha}$-$^{13}C^{\alpha}$ correlation map is not affected by expansion of the basis set. Nevertheless, since the torsional angles of conformers optimized at the 6-311++G(d,p) RHF level differ considerably from the torsional angles of conformers optimized at the 3-21G RHF level, the appropriate chemical shifts are different according to the sensitive torsional angle dependence of chemical shifts.

The Ala conformers also appear separately on $^{1}H^{\alpha}$-$^{13}C^{\alpha}$ maps, as seen in Figure 7. From this type of map the determination of conformer type is straightforward, and thus the type of the β-turn, as well as the position of the Ala residue can be determined unambiguously. This behavior does not change, as seen in Figure 8, when the β-turn is enlarged to include 4, 6, or 8 Ala residues (see also Figure 2).

As far as Val is concerned, the different conformers do not separate in the correlation map (Figure 9) as clearly as they do in case of Gly and Ala. Nevertheless, determination of the type of β-turn is straightforward from the $^{1}H^{\alpha}$-$^{13}C^{\alpha}$ map, and in

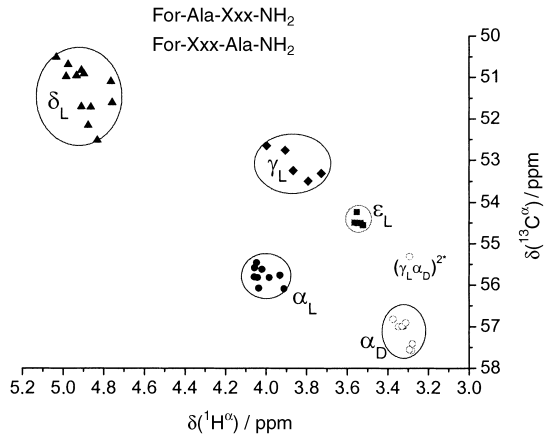

Figure 7. $^{1}H^{\alpha}$-$^{13}C^{\alpha}$ chemical-shift correlation map for Ala residues in both position.

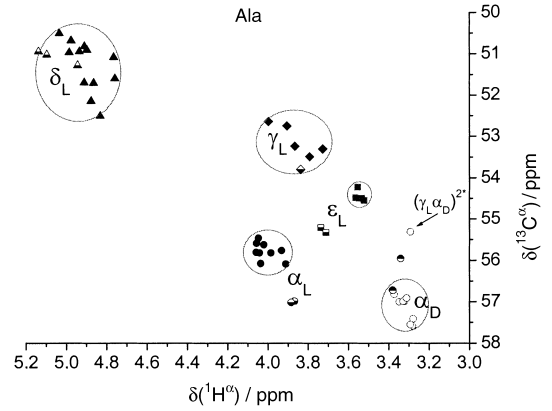

Figure 8. $^{1}H^{\alpha}$-$^{13}C^{\alpha}$ chemical-shift correlation map for Ala residues located in both positions of the β-turns of For-(L-Ala)$_n$-NH$_2$ models (n = 2, 4, 6 and 8). Half hollow symbols refer to n = 4, 6 and 8.

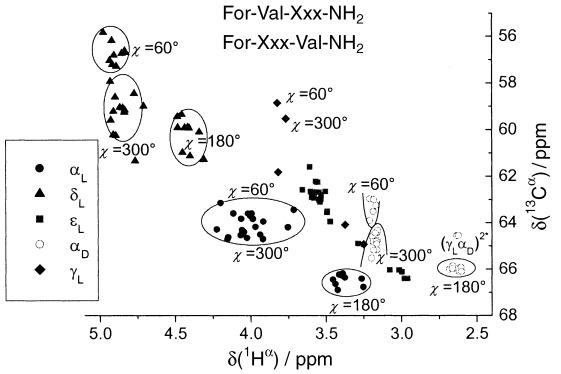

Figure 9. $^{1}H^{\alpha}$-$^{13}C^{\alpha}$ chemical-shift correlation map for Val residues in both position.

the case of type I β-turns, the position of the Val residue can clearly be assigned.

Furthermore, the side-chain orientation of the Val residue can also be determined. Conformers with $\chi \approx 60^{\circ}$ and 300° have the same $^{1}H^{\alpha}$, but different $^{13}C^{\alpha}$ chemical shift values with $\chi \approx 60^{\circ}$ having the smaller $^{13}C^{\alpha}$ shifts. Compared to $\chi \approx 60^{\circ}$ and 300° regions, the signals of $\chi \approx 180^{\circ}$ conformers always separate clearly, and are found at approximately 0.6–0.8 ppm smaller $^{1}H^{\alpha}$ values.

0947-6539/03/0905-1188 $ 20.00+.50/0 *Chem. Eur. J.* **2003**, *9*, No. 5

This side-chain effect separates the backbone conformers resulting in expanded backbone regions on the correlation maps. Subsequently, a side-chain region of one conformer can situate closely to a side-chain region of another conformer. Like on other chemical-shift/chemical-shift maps, regions of the ε_L and γ_L conformers appear to be elongated. Therefore, these regions may overlap with regions of other conformers. However, the effect of the χ torsional angle on chemical shifts can be clearly detected by examining correlation maps of For-Val-Xxx-NH_2 and For-Xxx-Val-NH_2 models separately (Figure 10). In case of For-Xxx-Val-NH_2 models (Figure 10B), the signals of the two conformers are far away from each other, consequently the determination of both backbone and side-chain conformers are straightforward.

The $^1H^{\alpha}$-$^{13}C^{\alpha}$ correlation map of the Ser residue is ambiguous as the signals of different conformers overlap with each other. The reason is the same as discussed for Val. The effect of side-chain orientation can be examined better on maps on which signals of residues in the first and the second position are plotted on different graphs (see Figure 11).

For both positions in the β-turn the signals of appropriate conformers are separated. Thus by virtue of NMR chemical shifts, the β-turn type can be determined. As observed for Val, the signals are separated better when Ser is in the second position; therefore the side-chain orientation can also be examined. For the Ser residue, the effects of both χ_1 and χ_2 torsional angles can be taken into account. The chemical shifts are clearly split due to the χ_1 torsional angle. Additionally, in the case of $\chi_1 \approx 300^\circ$ ($g-$ orientation), the sensitivity of chemical shifts to χ_2 torsional angle is also straightforward.

$^{13}C^{\alpha}$-$^1H^{\alpha}$-$^{13}C^{\beta}$ maps: Figure 12 clearly shows that for Ala, the conformers can be more clearly distinguished with the help of 3D correlation maps than with 2D maps. The $^{13}C^{\alpha}$-$^1H^{\alpha}$-$^{13}C^{\beta}$ map is especially useful for distinguishing the different side-chain conformers, as we can see it for Val in the $i+2$ position, in Figure 13. It must also be noted that with a properly chosen pulse sequence such 3D measurements can be performed.

$^{13}C^{\alpha}$-$^1H^{\alpha}$-$^{13}C'$ maps: Figure 14 shows for Ser in the $i+2$ position that the conformers clearly separate according to their χ_1 and χ_2 side-chain torsional angles. Therefore, if Ser is in the $i+2$ position, determination of the type of the β-turn and the side-chain orientation is straightforward by using this kind of correlation map.

It is also known that the chemical shifts of carbonyl carbons (C′) are due to the $-$I effect of the oxygen atom. The highest carbonyl carbon atom chemical shifts correspond to the $ag-$ orientation, because of strong hydrogen bonding between side-chain OH and C=O.

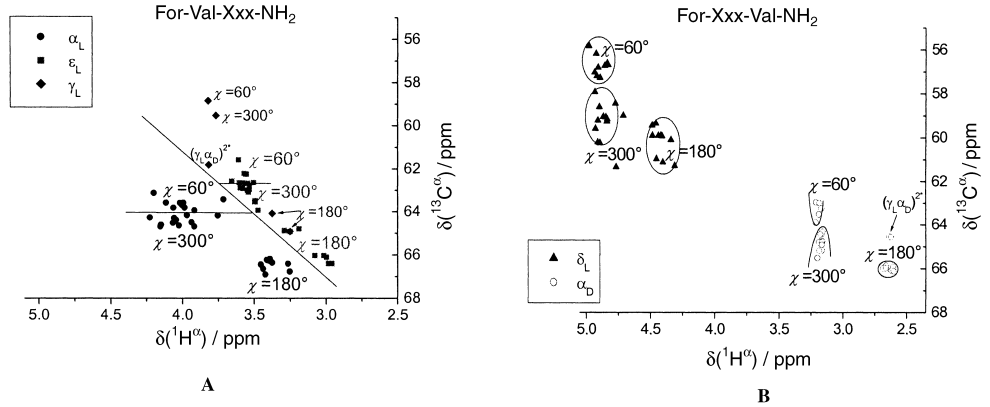

Figure 10. $^1H^{\alpha}$-$^{13}C^{\alpha}$ chemical-shift correlation maps [For–L–Val–Xxx–NH_2 (A) and For–Xxx–L–Val–NH_2 (B)] for Val residues.

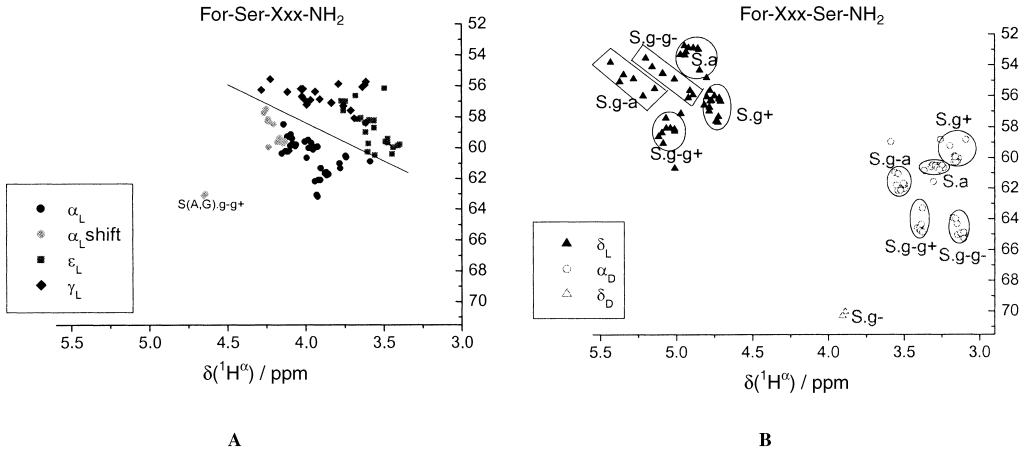

Figure 11. $^1H^{\alpha}$-$^{13}C^{\alpha}$ chemical-shift correlation maps [For–L–Ser–Xxx–NH_2 (A) and For–Xxx–L–Ser–NH_2 (B)] for Ser residues.

  0947-6539/03/0905-1189 $ 20.00+.50/0

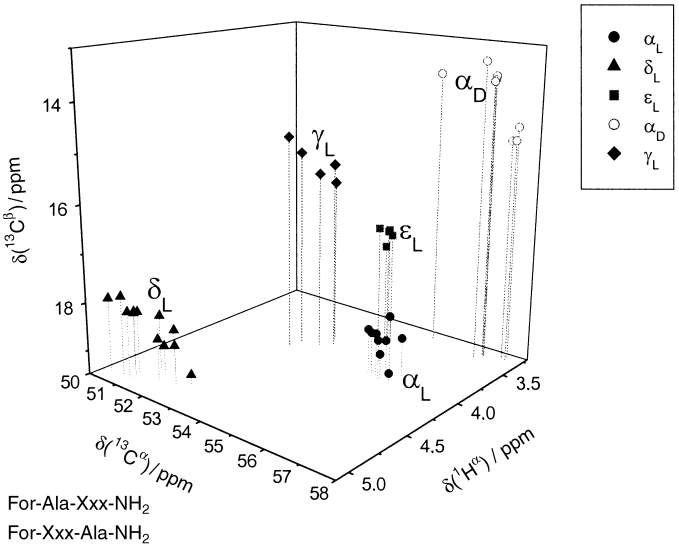

Figure 12. $^{13}C^{\alpha}$-$^{1}H^{\alpha}$-$^{13}C^{\beta}$ chemical-shift correlation map for Ala residues in both position.

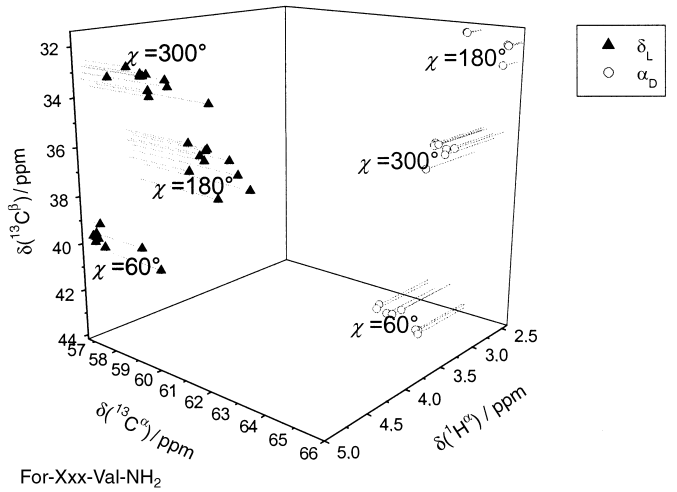

Figure 13. $^{13}C^{\alpha}$-$^{1}H^{\alpha}$-$^{13}C^{\beta}$ three-dimensional chemical-shift correlation map for Val residues in For–Xxx–L–Val–NH_2.

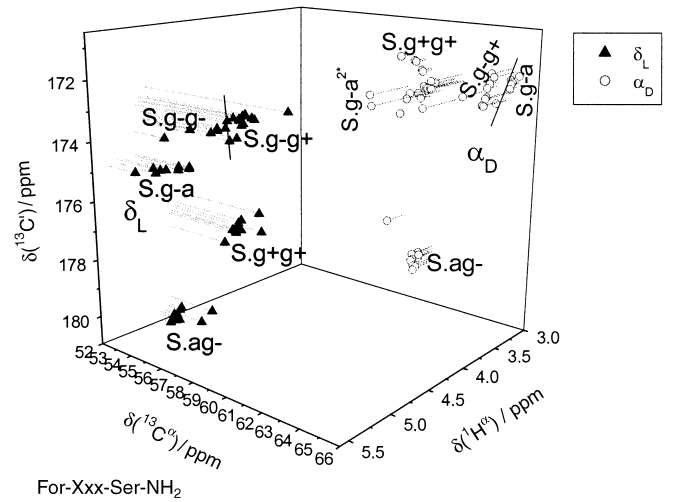

Figure 14. $^{13}C^{\alpha}$-$^{1}H^{\alpha}$-$^{13}C'$ chemical-shift correlation map for Ser residues in For–Xxx–L–Ser–NH_2.

Conclusion

Establishing correlation between peptide main-chain folds and chemical shifts provides a continuous challenge for experimentalists and theoreticians alike. For theoreticians, uncertainties arise, for example, from the problem of ideal size and type of a peptide model to be used for the computations, the required minimum level of ab initio theory, and the incorporation of important structural factors. There are just as severe experimental difficulties in establishing such correlations. Consequently, unambiguous correlations have been put forward only for the α-helical and β-sheet regions of the Ramachandran surface. One of the principal aims of this computational study has been the confirmation of existing correlations and derivation of new ones for selected dipeptides as models of type I and type II β-turns. Some important findings of this study, relevant or related to this issue, are as follows:

- The model chosen for the present computations, For-Xxx-Yyy-NH_2, with Xxx and Yyy = Gly, Ala, Val, and Ser is adequate, as proven by NMR chemical shift calculations on For-(L-Ala)$_n$-NH_2 ($n = 4$, 6, 8) model systems. Larger systems exhibit the same overall behavior as the smaller models.
- The four residues, Gly, Ala, Val, and Ser model adequately the conformational characteristics of natural β-turns, since Gly and Ser are often found in the second position of type II and type I β-turns, respectively, while in the first position hydrophobic residues, such as Val, are abundant.
- The TZ2P GIAO-DFT(B3LYP) level of theory, employed extensively in this study, is the best compromise between accuracy and computational effort, as shown by calculations up to the GIAO-CCSD(T) level. The adequacy of the computed chemical shifts is also shown by comparison with data deposited in the BMRB database, and with experimental values of Wishart.
- Chemical shift differences between conformers of the same residue can be traced back mainly to differences in dihedral angles, as shown on chemical-shift/chemical-shift plots by employing idealized conformers with constrained ϕ, ψ, and χ dihedral angles.
- One-dimensional chemical-shift/dihedral-angle plots do not provide sufficient information to distinguish between spatial orientations. On the other hand, two- and three-dimensional chemical-shift/chemical-shift plots allow unambiguous determination of backbone, and even side-chain conformations. This study seems to indicate, that for this purpose, the two-dimensional $^{1}H^{\alpha}$-$^{13}C^{\alpha}$, the three-dimensional $^{13}C^{\alpha}$-$^{1}H^{\alpha}$-$^{13}C'$, and the $^{13}C^{\alpha}$-$^{1}H^{\alpha}$-$^{13}C^{\beta}$ correlation maps are the most useful.

In summary, ab initio isotropic NMR shielding results presented in this paper, for dipeptide systems modeling β-turns, facilitate and encourage the application of correlated relative chemical-shift information from ^{1}H-^{13}C HSQC, HNCA, HNCB, and other multiple-pulse NMR experiments to extract structural information *directly* from these measurements. This opens an alternative route to NOE's for the derivation of protein structures from their NMR spectra.

Therefore, the usefulness of the approach of direct determination of conformations of protein building units from

0947-6539/03/0905-1190 $ 20.00+.50/0 *Chem. Eur. J.* **2003**, *9*, No. 5

multidimensional NMR experiments depends on what effect the side chains, solvation, anisotropic factors, and inter- and intramolecular hydrogen bonding might have on the relative chemical shifts of the selected nuclei. Detailed theoretical investigations of more model compounds and more correlated chemical-shielding plots are needed to establish the magnitude of these effects, while it is also hoped that the present theoretical results will encourage experimental work in this direction.

Acknowledgement

The research described was supported by grants from the Hungarian Scientific Research Fund (OTKA T033074 and OTKA T032486).

[1] IUPAC-IUB Commission on Biochemical Nomenclature Biochemistry **1970**, *9*, 3471.
[2] F. C. Bernstein, T. F. Koetyle, G. J. B. Williams, E. F. Meyer, M. D. Brice, Jr, J. R. Rodgers, O. Kennard, T. Shimanouchi, M. Tasumi, *J. Mol. Biol.* **1977**, *112*, 535.
[3] http://www.rcsb.org/pdb/.
[4] D. Neuhaus, M. Williamson, *The Nuclear Overhauser Effect in Structural and Conformational Analysis*, VCH, New York, **1989**.
[5] a) K. Wüthrich, in *NMR of Protein and Nucleic Acids,* Wiley, New York, **1986**; b) K. Wüthrich, *Science* **1989**, *243*, 45.
[6] J. A. Smith, L. G. Pease, *CRC Crit. Rev. Biochem.* **1980**, *8*, 315.
[7] a) M. Nilges, *J. Mol. Biol.* **1995**, *245*, 645; b) J. Cavanagh, W. J. Fairbrother, A. G. Palmer III, N. J. Skelton, *Protein NMR Spectroscopy. Principles and Practice*, Academic Press, San Diego, **1996**.
[8] S. W. Fesik, E. R. P. Zuiderweg, *Q. Rev. Biophys* **1990**, *23*, 97.
[9] G. M. Clore, A. M. Gronenborn, *Prog. Nucl. Magn. Reson. Spectrosc.* **1991**, *23*, 43.
[10] A. Bax, S. Grzesiek, *Acc. Chem. Res.* **1993**, *26*, 131.
[11] a) D. S. Wishart, B. D. Sykes, *J. Mol. Biol.* **1991**, *222*, 311; b) *Methods in Enzimology* (Eds: T. L. James, N. J. Oppenheimer) D. S. Wishart, B. D. Sykes, Academic Press, New York, **1992**.
[12] L. Szilágyi, *Prog. Nucl. Magn. Reson. Spectrosc.* **1995**, *27*, 325.
[13] B. Celda, C. Baimonti, M. J. Arnau, R. Tejero, G. T. Montelione, *J. Biomol. NMR* **1885**, *5*, 161.
[14] H. Saito, *Magn. Reson. Chem.* **1986**, *24*, 835, and references therein.
[15] C. E. Johnson, F. A. Bovey, *J. Chem. Phys.* **1958**, *29*, 1012.
[16] a) S. J. Perkins, K. Wüthrich, *Biochim. Biophys. Acta* **1979**, *576*, 409; b) C. W. Haigh, R. B. Mallion, *Prog. Nucl. Magn. Reson. Spectrosc.* **1980**, *13*, 303; c) M. P. Williamson, *Biopolymers* **1990**, *29*, 1423; d) S. A. Spera, A. Bax, *J. Am. Chem. Soc.* **1991**, *113*, 5490.
[17] J. Augspurger, J. G. Pearson, E. Oldfield, C. E. Dykstra, K. D. Park, D. Schwartz, *J. Magn. Reson.* **1992**, *100*, 342.
[18] a) J. Gluska, M. Lee, S. Coffin, D. Cowburn, *J. Am. Chem. Soc.* **1989**, *111,* 7716; b) J. Gluska, M. Lee, S. Coffin, D. Cowburn, *J. Am. Chem. Soc.* **1990**, *112*, 2843
[19] C. M. Santiveri, M. Rico, M. A. Jimenez, *J. Biomol. NMR* **2001**, *19*, 331.
[20] Le, E. Oldfield, *J. Biomol. NMR* **1994**, *4*, 341.
[21] a) A. C. de Dios, J. G. Pearson, E. Oldfield, *Science* **1993**, *260*, 1491; b) A. C. de Dios, J. G. Pearson, E. Oldfield, *J. Am. Chem. Soc.* **1993**, *115*, 9768; c) A. C. de Dios, E. Oldfield, *J. Am. Chem. Soc.* **1994**, *116*, 5307; d) H. B. Le, J. G. Pearson, A. C. de Dios, E. Oldfield, *J. Am. Chem. Soc.* **1995**, *117*, 3800.
[22] A. Perczel, A. G. Császár, *J. Comput. Chem.* **2000**, *21*, 882.
[23] A. Perczel, A. G. Császár, *Chem. Eur. J.* **2001**, *7*, 1069.
[24] A. Perczel, A. G. Császár, *Eur. Phys. J. D* **2002**, *20*, 513.
[25] a) H. M. Sulzbach, P. von R. Schleyer, H. F. Schaefer III, *J. Am. Chem. Soc.* **1994**, *116*, 3967; b) H. M. Sulzbach, P. von R. Schleyer, H. F. Schaefer III, *J. Am. Chem. Soc.* **1995**, *117*, 2632; c) H. M. Sulzbach, G. Vacek, P. R. Schreiner, J. M. Galbraith, P. von R. Schleyer, H. F. Schaefer III, *J. Comput. Chem.* **1997**, *18*, 126.
[26] H. Le, E. Oldfield, *J. Phys. Chem.* **1996**, *100*, 16423.
[27] D. Jiao, M. Barfield, V. J. Hruby, *J. Am. Chem. Soc.* **1993**, *115*, 10883.
[28] N. R. Luman, M. P. King, J. D. Augspurger, *J. Comput. Chem.* **2001**, *22*, 366.
[29] a) B. R. Seavey, E. A. Farr, W. M. Westler, J. L. Markley, *J. Biomol. NMR* **1991**, *1*, 217; b) www.bmrb.wisc.edu
[30] a) L. Müller, *J. Am. Chem. Soc.* **1979**, *101*, 4481; b) A. Bax, R. H. Griffey, B. L. Hawkins, *J. Magn. Reson.* **1983**, *55*, 301; c) A. G. Redfield, *Chem. Phys. Lett.* **1987**, *96*, 537.
[31] G. Bodenhausen, D. J. Ruben, *Chem. Phys. Lett.* **1980**, *69*, 185.
[32] M. Ikura, L. E. Kay, A Bax, *Biochemistry* **1990**, *29*, 4659.
[33] N. Asakawa, H. Kurosu, I. Ando, A. Shoji, T. Ozaki, *J. Mol. Struct. (THEOCHEM)* **1994**, *317*, 119.
[34] A. C. de Dios, E. Oldfield, *J. Am. Chem. Soc.* **1994**, *116*, 11485.
[35] G. Zheng, L. M. Wang, J. Z. Hu, X. D. Zhang, L. F. Shen, C. H. Ye, G. A. Webb, *Magn. Reson. Chem.* **1997**, *35*, 606.
[36] D. D. Laws, H. B. Le, A. C. de Dios, R. H. Havlin, E. Oldfield, *J. Am. Chem. Soc.* **1995**, *117*, 9542.
[37] W. Gronwald, L. Willard, T. Jellard, R. F. Boyko, K. Rajarathnam, D. S. Wishart, F. D. Sonnichsen, B. D. Sykes, *J. Biomol. NMR* **1998**, *12*, 395.
[38] G. Cornilescu, F. Delaglio, A. Bax, *J. Biomol NMR.* **1999**, *13*, 289.
[39] J. G. Pearson, J. F. Wang, J. L. Markley, H. B. Le, E. Oldfield, *J. Am. Chem. Soc.* **1995**, *117*, 8823.
[40] R. H. Havlin, H. B. Le, D. D. Laws, A. C. de Dios, E. Oldfield, *J. Am. Chem. Soc.* **1997**, *119*, 11951.
[41] J. G. Pearson, H. B. Le, L. K. Sanders, N. Godbout, R. H. Havlin, E. Oldfield, *J. Am. Chem. Soc.* **1997**, *119*, 11941.
[42] C. Venkatachalam, *Biopolymers* **1968**, *6*, 1425.
[43] a) M. Levitt, *J. Mol. Biol.* **1976**, *104*, 59; b) P. Y. Chou, G. D. Fasman, *J. Mol. Biol.* **1977**, *115*, 135.
[44] A. G. Császár, A. Perczel, *Prog. Biophys. Mol. Biol.* **1999**, *71*, 243.
[45] A. Perczel, I. Jákli, I. G. Csizmadia, unpublished results.
[46] Gaussian 98 (Revision A.5), M. J. Frisch, G. W. Trucks, H. B. Schlegel, G. E. Scuseria, M. A. Robb, J. R. Cheeseman, V. G. Zakrzewski, J. A. Montgomery, R. E. Stratmann, J. C. Burant, S. Dapprich, J. M. Millam, A. D. Daniels, K. N. Kudin, M. C. Strain, O. Farkas, J. Tomasi, V. Barone, M. Cossi, R. Cammi, B. Mennucci, C. Pomelli, C. Adamo, S. Clifford, J. Ochterski, G. A. Petersson, P. Y. Ayala, Q. Cui, K. Morokuma, D. K. Malick, A. D. Rabuck, K. Raghavachari, J. B. Foresman, J. Cioslowski, J. V. Ortiz, B. B. Stefanov, G. Liu, A. Liashenko, P. Piskorz, I. Komaromi, R. Gomperts, R. L. Martin, D. J. Fox, T. Keith, M. A. Al-Laham, C. Y. Peng, A. Nanayakkara, C. Gonzalez, M. Challacombe, P. M. W. Gill, B. G. Johnson, W. Chen, M. W. Wong, J. L. Andres, M. Head-Gordon, E. S. Replogle, J. A. Pople, Gaussian, Inc., Pittsburgh, PA, **1998**.
[47] See www.python.org.
[48] T. M. Wonnacott, R. J. Wonnacott, *Introductory Statistics*, 5th ed, Wiley, New York, **1990**.
[49] J. F. Stanton, J. Gauss, J. D. Watts, W. J. Lauderdale, R. J. Bartlett, *Int. J. Quantum Chem. Symp.* **1992**, *26*, 879.
[50] R. Ditchfield, *Mol Phys.* **1974**, *27*, 789.
[51] K. Wolinski, J. F. Hinton, P. Pulay, *J. Am. Chem. Soc.* **1990**, *111*, 8251.
[52] a) A. D. Becke, *Phys. Rev. A* **1988**, *38*, 3098; b) C. Lee, W. Yang, R. G. Parr, *Phys. Rev. B* **1988**, *37*, 785.
[53] J. Gauss, *J. Chem. Phys.* **1993**, *99*, 3629.
[54] J. Gauss, J. F. Stanton, *J. Chem. Phys.* **1995**, *102*, 251.
[55] J. Gauss, J. F. Stanton, *J. Chem. Phys.* **1996**, *104*, 2574.
[56] R. Krishnan, J. S. Binkley, R. Seeger, J. A. Pople, *J. Chem. Phys.* **1980**, *72*, 650.
[57] A. Schafer, H. Horn, R. Ahlrichs, *J. Chem. Phys.* **1992**, *97*, 2571.
[58] A. Schafer, C. Huber, R. Ahlrichs, *J. Chem. Phys.* **1994**, *100*, 5829.
[59] A. G. Császár, W. D. Allen, H. F. Schaefer III, *J. Chem. Phys.* **1998**, *108*, 9751.
[60] D. S. Wishart, B. D. Sykes, F. M. Richards, *J. Mol. Biol.* **1991**, *222*, 311–333.
[61] A. Perczel, M. A. McAllister, P. Császár, I. G. Csizmadia, *J. Am. Chem. Soc.* **1993**, *115*, 4849.

Received: August 14, 2002 [F4345]

  0947-6539/03/0905-1191 $ 20.00+.50/0